

trol system (TCS), the spectrometer control, and the *Pegasus gui*. At the end of this period it was possible through *Pegasus* to track and map a source using all three spectrometers simultaneously. The upgrade project will be finished during the second half of 1998, after which the new system will be in use.

### 3. The Future

During 1999, SEST will be equipped with a nutating subreflector, designed and built at IRAM (Institut de Radio Astronomie Millimétrique). This will be slightly smaller than the present subreflector and be insensitive to ground radiation spilling over the primary mirror. It

means, however, that the telescope focal-ratio will be changed, necessitating a redesign of some of the receiver optics. The new subreflector will make it possible to use one of the new-generation bolometer arrays which, for reasons concerning the uniform illumination of all pixels, can only satisfactorily be operated with such a subreflector. Therefore, in 1999, we will install a 37-channel bolometer array receiver working at a wavelength of 1.3 mm. This will be built by Ernst Kreysa at the Max-Planck-Institut für Radioastronomie in Bonn, with support from the Astronomical Institute of the Ruhr-Universität Bochum and Onsala Space Observatory. Mapping will become much faster due to the large number of channels. The

efficiency for mapping extended sources as well as for observations of point-like sources will also increase, because the sky noise added by the atmosphere is correlated between the channels and can thus be eliminated. This implies that it will be possible to work at the detector noise level even in marginal atmospheric conditions.

We also expect that the on-the-fly mapping mode will be available at the end of these upgrades. This is a fast mapping mode during which data is taken continuously while the telescope is scanning across a source, and thus the total mapping time will be decreased by at least a factor of three.

During 1999, SEST will also take delivery of a digital autocorrelation spectrometer (ACS) which will be built at the Australia Telescope National Facility as part of the new Swedish-Australian collaboration. It will have selectable bandwidths decreasing from 1 GHz to 64 MHz by factors of 2 and 2048 frequency channels. This will provide a flexible alternative to the AOS, but it will also be possible to use the AOS and ACS at the same time with different bandwidths.

Further into the future it is foreseen that an SIS heterodyne array receiver, working in the 1.3-mm window with up to 16 elements, will be installed at SEST. This also means that 16 spectrometers will have to be used in combination with the receiver, and thus the present spectrometers will have to be replaced, possibly through the Swedish-Australian collaboration.

L.-Å. Nyman  
lnyman@puppis.ls.eso.org

## Molecular Lines in Absorption at High Redshift

F. COMBES, *Observatoire de Paris, DEMIRM, Paris, France*

T. WIKLIND, *Onsala Space Observatory, Onsala, Sweden*

### Abstract

Molecular absorption lines at high redshift (0.2 to 1) were discovered a few years ago, and they revealed a very precious tool for many purposes. They allow the detection of many molecules, and in particular those not observable from the ground at  $z = 0$ . such as water and molecular oxygen. The excitation temperature of molecules are often close to that of the cosmic background radiation, and can serve to measure it as a function of redshift. The absorption comes frequently from a gravitational lens in front of a quasar, so that they help to determine time-delays and the Hubble constant. The high spectral resolution of radio observations allows to put constraints on the variation of the fine-structure constant over a large frac-

tion of the Hubble time. With the next-generation millimetre interferometers, many such systems would be observable, which will allow the exploration of young galaxies in the Universe.

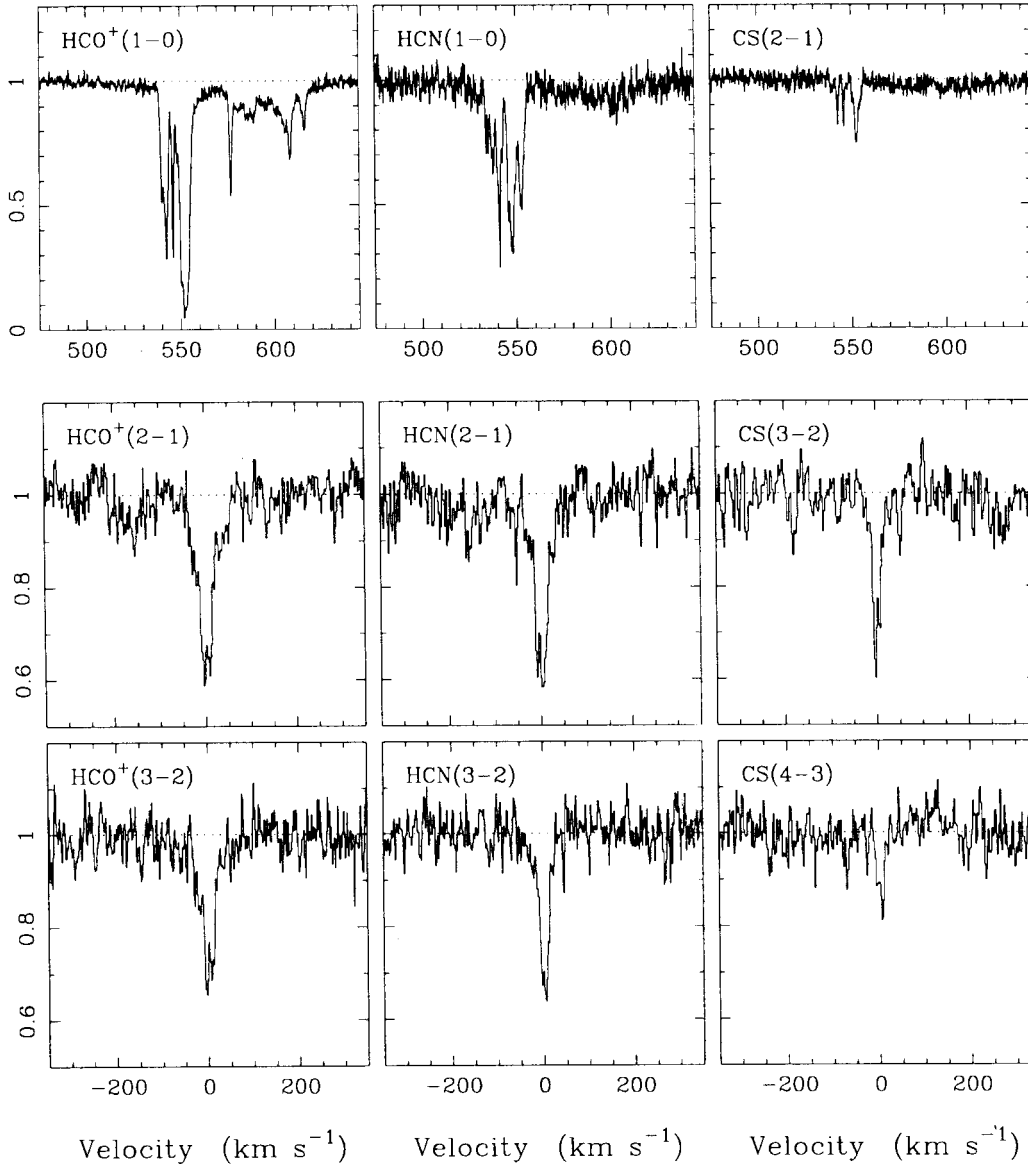
### 1. Background

Absorption lines are a sensitive probe for studying the interstellar medium. Especially in distant objects, where emission lines become diluted with distance squared, whereas the detectability of absorption lines only depends on the observed flux of the background source. This is well known from optical spectroscopy, where the combination of sensitive detectors and large telescopes allows observation of very tenuous gas towards distant background QSO. In principle, absorption of molecular rotational lines

can be used to probe the densest and coldest part of the ISM in distant galaxies, much in the same way as optical lines probe the warm and diffuse gas. Since new stars are formed in molecular clouds, a study of this ISM component traces the star-formation conditions and its history in galaxies. There are, however, several difficulties associated with the detection of such lines and it was not before 1993 that the first distant molecular absorption line system was detected. Since then a total of four such systems at redshifts between  $z = 0.2-0.9$  have been observed.

### 2. Discovery of Molecular Absorption-line Systems

The 15-m Swedish-ESO Submillimetre Telescope (SEST) on La Silla has



Cen A  
D=4 Mpc

PKS1830-211  
D=4 Gpc

Figure 1:  $\text{HCO}^+$ , HCN and CS absorption lines towards the nearby Cen A ( $D \approx 4$  Mpc) and PKS1830-211 ( $D \approx 4$  Gpc). For PKS1830-211 two different rotational transitions are shown for each molecule. This illustrates that the detectability of molecular absorption lines does not depend on distance but on the column density and strength of the background continuum source.

played a crucial role in the study of molecular absorption-line systems. The first such systems was detected with the SEST at Christmas time 1993 (Wiklind & Combes, 1994). The most distant molecular absorption line system ( $z = 0.9$ ) was also detected with the SEST (Wiklind & Combes, 1996a). In the former case (PKS1413+135), the redshift of the absorbing gas was known from both optical spectra and 21 cm HI absorption, occurring at  $z = 0.247$  (Carilli et al., 1992). The molecular absorption line, the CO(1-0) transition, turned out to be so narrow that it could easily have been mistaken for a bad channel in the spectrometer. Observations of additional molecules and using higher spectral resolution showed, however, that the absorption was indeed real. In the latter case (PKS 1830-211), nothing was known about the redshift. The background radio source was suspected to be a gravitational lens (Subrahmanyan et al., 1990), but with no optical counterpart. As such it was a good candidate for molecular absorption. Millimetre wave

receivers are characterised by a narrow bandwidth but a high spectral resolution (typically  $\leq 1$  GHz and 0.1 MHz, respectively). Nevertheless, in the case of PKS 1830-211 we scanned the 3-mm band in frequency until we encountered an absorption line (cf. *The Messenger* 84, p. 23). After some guessing at its identity, we found several additional absorption lines and could determine the redshift of the absorber to be  $z = 0.88582$ . To date we have detected four molecular absorption-line systems (see Table 1). Some systems include several velocity components.

These molecular absorption objects are the continuation at high column densities ( $10^{21}$ – $10^{24}$   $\text{cm}^{-2}$ ) of the whole spectrum of absorption systems, from the Ly $\alpha$  forest ( $10^{12}$ – $10^{19}$   $\text{cm}^{-2}$ ) to the damped Ly $\alpha$  and HI 21 cm absorptions ( $10^{19}$ – $10^{21}$   $\text{cm}^{-2}$ ). It is currently thought that the Ly $\alpha$  forest originates from gaseous filaments in the extra-galactic medium, that the damped and HI absorptions involve mainly the outer parts of spiral galaxies. The molecular absorp-

tions concern the central parts of galaxies.

Among the four detected systems, there are two cases of confirmed gravitational lenses, with multiple images (the two other cases are likely to be internal absorption). This is not surprising, since detection of molecular absorption requires that the line of sight to the background QSO must pass close to the centre of an intervening galaxy. The surface density is then larger than the critical one for multiple images. In the present two cases (B0218+357 and PKS 1830-211), the separation between the two images is small enough that only a galaxy bulge is required for the lensing.

#### *Detectability of Molecular Absorption Lines*

In addition to the four detected molecular absorption-line systems we have undertaken a systematic survey of about a hundred candidates, selected from flat-spectrum continuum sources. The continuum needs to be at least 0.2

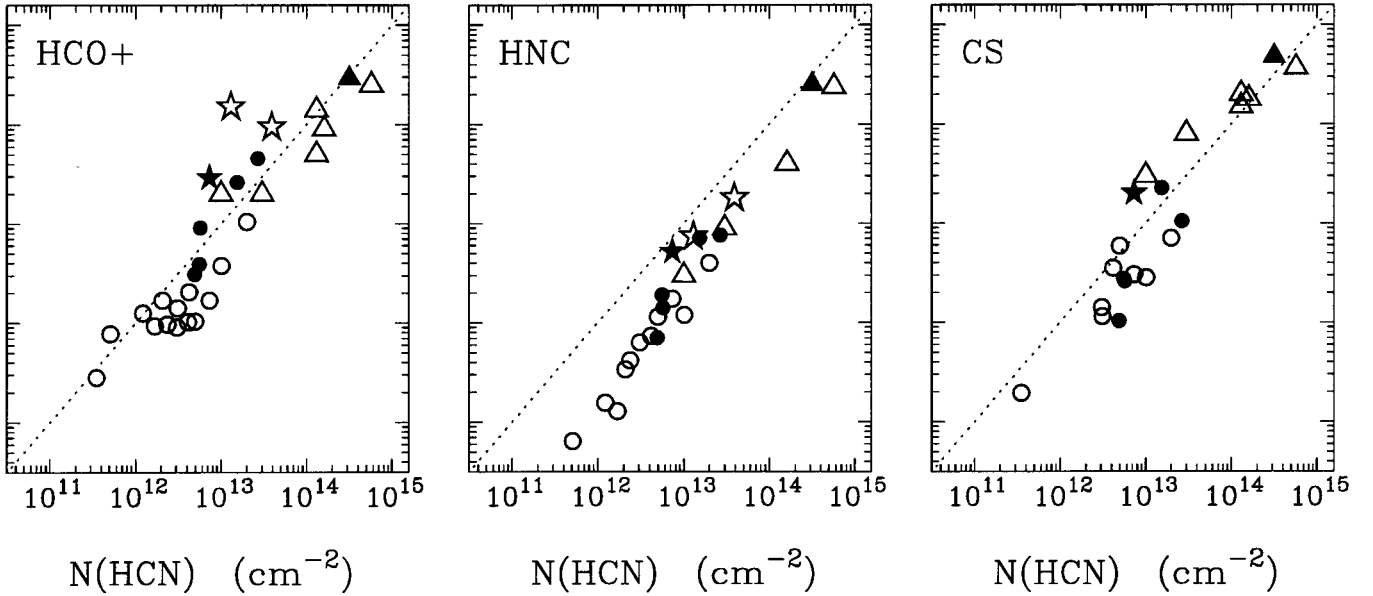


Figure 2: Comparison of column densities for various molecules and absorption systems. Open circles are Galactic diffuse clouds (Lucas & Liszt, 1996), open triangles somewhat denser Galactic clouds seen towards the galactic centre (Greaves & Nyman, 1996), filled circles represent absorption in Cen A (Wiklind & Combes, 1997a). The distant absorption systems are represented by open stars (B1504+377), filled stars (PKS1413+135), filled triangle (PKS1830-211). B0218+357 is too saturated to allow reliable column density estimates. The dotted line represents a one-to-one correspondence and is not a fit to the data.

Jy to allow detection of intervening molecular gas<sup>1</sup>. The redshift of the absorbing candidate is known, either from previously detected HI absorption; 21 cm or damped Ly $\alpha$ , which is the case for PKS1413+135 and B0218+357 (Wiklind & Combes, 1994, 1995) or from optical line emission of a galaxy on the line of sight to a radio source; B1504+377 (Wiklind & Combes, 1996b). When the continuum source is strong enough, at least 1 Jy, and no redshift is known, it is possible to search for absorption lines by scanning in frequency in a manner similar to what was done for PKS 1830-211. This last method is the most promising with the new-generation millimetre instruments, that will gain an order of magnitude in sensitivity. Indeed, the best candidates are the most obscured ones, where no redshift is available.

<sup>1</sup>This limit is set by the sensitivity of today's millimetre wave telescopes to point like continuum sources and scales as the total collecting surface area.

The utility of molecular absorption lines comes from the high sensitivity. First of all, the observed property is the velocity integrated opacity, which is directly proportional to the square of the permanent electric dipole moment. This means that a molecule like HCO<sup>+</sup>, which is  $\sim 10^{-4}$  less abundant than CO, but has a dipole moment  $\sim 10^2$  times larger than that of CO, can be as easily observed. Secondly, the small extent of the background continuum source means that there is no distance dependence, the sensitivity only depending on the observed background flux. Molecular absorption lines are as easy to detect at  $z \approx 0$  as at  $z = 1$ , except that at small distances emission can make absorption-line measurements more difficult. To illustrate this we show in Figure 1 HCO<sup>+</sup>, HCN and CS absorption from Cen A at a distance of  $\sim 4$  Mpc (Wiklind & Combes, 1997a) and from PKS 1830-211 at a distance of  $\sim 4000$  Mpc (Wiklind & Combes, 1996a). Both sets of spectra have been obtained with the SEST.

### 3. Results on Molecular Abundances

About 15 different molecules have been detected in absorption at high redshifts, in a total of 30 different transitions. This allows a detailed chemical study and comparison with local clouds. In Figure 2 we show such a comparison between our high redshift absorption line systems and Galactic absorption (Cen A is also included). The dispersion in column densities reflects the dispersion in molecular cloud properties. The high redshift systems do not appear to be different from local ones, suggesting that the conditions for star formation are the same up to  $z \sim 1$  as at the present.

#### *Molecules Unobservable from the Ground at $z = 0$*

A particular interest comes from transitions that were never detected before. Because of atmospheric absorption in the H<sub>2</sub>O and O<sub>2</sub> lines, it is impossible to have a correct estimation of the abun-

Table 1. Properties of molecular absorption line systems

Source	$z_a^a$	$z_e^b$	$N_{CO}$ cm <sup>-2</sup>	$N_{H_2}$ cm <sup>-2</sup>	$N_{HI}$ cm <sup>-2</sup>	$A'_v^c$	$N_{HI} / N_{H_2}$
Cen A	0.00184	0.0018	$1.0 \times 10^{16}$	$2.0 \times 10^{20}$	$1 \times 10^{20}$	50	0.5
PKS1413+357	0.24671	0.247	$2.3 \times 10^{16}$	$4.6 \times 10^{20}$	$1.3 \times 10^{21}$	2.0	2.8
B31504+377A	0.67335	0.673	$6.0 \times 10^{16}$	$1.2 \times 10^{21}$	$2.4 \times 10^{21}$	5.0	2.0
B31504+377B	0.67150	0.673	$2.6 \times 10^{16}$	$5.2 \times 10^{20}$	$< 7 \times 10^{20}$	$< 2$	$< 1.4$
B0218+357	0.68466	0.94	$2.0 \times 10^{19}$	$4.0 \times 10^{23}$	$4.0 \times 10^{20}$	850	$1 \times 10^{-3}$
PKS 1830-211A	0.88582	?	$2.0 \times 10^{18}$	$4.0 \times 10^{22}$	$5.0 \times 10^{20}$	100	$1 \times 10^{-2}$
PKS 1830-211B	0.88489	?	$1.0 \times 10^{16d}$	$2.0 \times 10^{20}$	$1.0 \times 10^{21}$	1.8	5.0
PKS 1830-211C	0.19267	?	$< 6 \times 10^{15}$	$< 1 \times 10^{20}$	$2.5 \times 10^{20}$	$< 0.2$	$> 2.5$

<sup>a</sup>Redshift of absorption line. – <sup>b</sup>Redshift of background source. – <sup>c</sup>Extinction corrected for redshift using a Galactic extinction law. – <sup>d</sup>Estimated from the HCO<sup>+</sup> column density of  $1.3 \times 10^{13}$  cm<sup>-2</sup>. – <sup>e</sup>21cm HI data taken from Carilli et al., 1992, 1993, 1998.

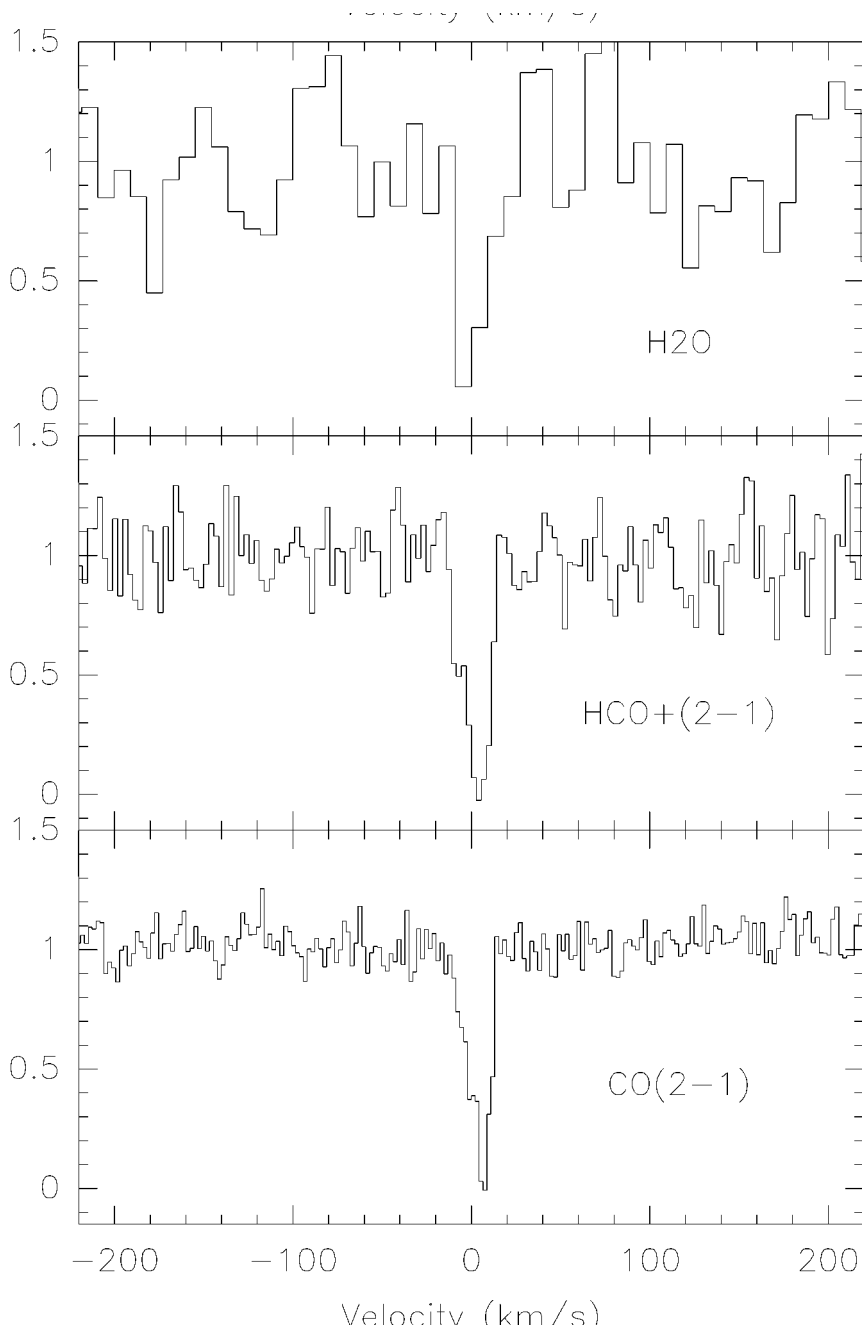


Figure 3: Spectrum of ortho-water in its fundamental line at 557 GHz, redshifted at 331 GHz, in absorption towards B0218+357. The line has the same width as the previously detected  $\text{HCO}^+(2-1)$  and  $\text{CO}(2-1)$  lines. The velocity resolution is 9.1, 2.8 and 2.2 km/s from top to bottom. All spectra have been obtained with the IRAM 30-m telescope, and normalised to the continuum level.

dances of these two molecules in the local interstellar medium. But these are key elements of interstellar chemistry. The redshift of the distant molecular absorption-line systems shifts the frequency of these lines into atmospheric windows observable from the ground. The highest column density systems (B0218+357 and PKS1830-211) are privileged targets to try to detect these fundamental molecules (e.g. Combes & Wiklind, 1995, 1996).

**Water.** We have chosen the absorbing cloud in front of B0218+357, where already optically thick lines of CO,  $^{13}\text{CO}$  and  $\text{C}^{18}\text{O}$  have been detected (Combes & Wiklind, 1995). The optical depth of

the  $\text{CO}(2-1)$  line was derived to be  $\sim 1500$ , and therefore the  $\text{H}_2$  column density around  $5 \cdot 10^{23}$  to  $10^{24} \text{ cm}^{-2}$ . At  $z = 0.68466$ , the fundamental ortho transition of water at 557 GHz is redshifted to 331 GHz into an atmospheric window.

According to models, the  $\text{H}_2\text{O}/\text{H}_2$  abundance ratio is expected between  $10^{-7}$  and  $10^{-5}$ , and observations of isotopic lines in molecular clouds of the Milky Way, such as  $\text{H}_2^{18}\text{O}$  and  $\text{HDO}$ , have confirmed these expectations. It was thought until recently that these abundances concerned only the neighbourhood of star-forming regions, such as the Orion hot core, where water ice is evaporated from grains. However, Cer-

nicharo et al. (1997) detected with the ISO satellite water in absorption at  $179 \mu$  in front of SgrB2, and this revealed that cold water was ubiquitous.

Our detection with the IRAM 30-m telescope of ortho-water in its fundamental line at 557 GHz confirms this result. The line is highly optically thick, and has about the same width as the other optically thick lines detected in absorption in this cloud (see Fig. 3). If the excitation temperature was high (as in the Orion hot core), we would have expected to detect also the excited line at 183 GHz (redshifted at 109 GHz). An upper limit on this line gives us an upper limit on  $T_{\text{ex}}$  of 10–15K, and an estimation of the optical depth of the 557 GHz line of  $\sim 40,000$  (Combes & Wiklind, 1997). This leads to an  $\text{H}_2\text{O}/\text{H}_2$  abundance ratio of  $10^{-5}$ , in the upper range of expected values.

**Molecular oxygen.** As an element, oxygen is about twice as abundant as carbon ( $\text{O}/\text{H} \sim 8.5 \cdot 10^{-4}$ ), meaning that at most half of the oxygen atoms can be used to make CO. The other half can be found in the form of atomic oxygen (O), or molecules:  $\text{O}_2$ , OH and  $\text{H}_2\text{O}$ . Since OH and  $\text{H}_2\text{O}$  are much less abundant than CO, in dense molecular clouds, we expect  $\text{O}_2$  to be about as abundant as CO. Until recently, the upper limits on the  $\text{O}_2/\text{CO}$  ratio was 0.1, from observations of the isotopic line  $\text{O}^{18}\text{O}$  and the direct  $\text{O}_2$  in emission in remote starbursts. The upper limits obtained through absorption lines are more reliable, since they involve only one individual molecular cloud, where  $\text{O}_2$  is not photo-dissociated.

We have searched for many  $\text{O}_2$  lines with various millimetre telescopes (SEST 15 m, IRAM 30 m, Kitt-Peak 12 m, Green-Bank 43 m and Nobeyama 45 m). All these searches resulted in an upper limit of  $\text{O}_2/\text{CO} < 2 \cdot 10^{-3}$  at  $1\sigma$  (Combes et al., 1997). This is much below theoretical expectations and suggests that oxygen is frozen on to dust grains, or that steady-state chemistry is never reached. In the latter case, most of the oxygen would remain atomic even in dense molecular clouds.

#### 4. Time-Delay and the Hubble Constant

It is well known that gravitational lenses provide an original method to derive the Hubble constant, in allowing an absolute determination of the distance of a source, for which the redshift is known. Imagine that we observe two images of a quasar through a gravitational lens, and let us call  $d_1$  and  $d_2$  the corresponding lengths of the light paths to these two images. If we measure the time lag between the moment when a burst of light appears on one image and the moment where the same burst appears on the other, we can deduce the

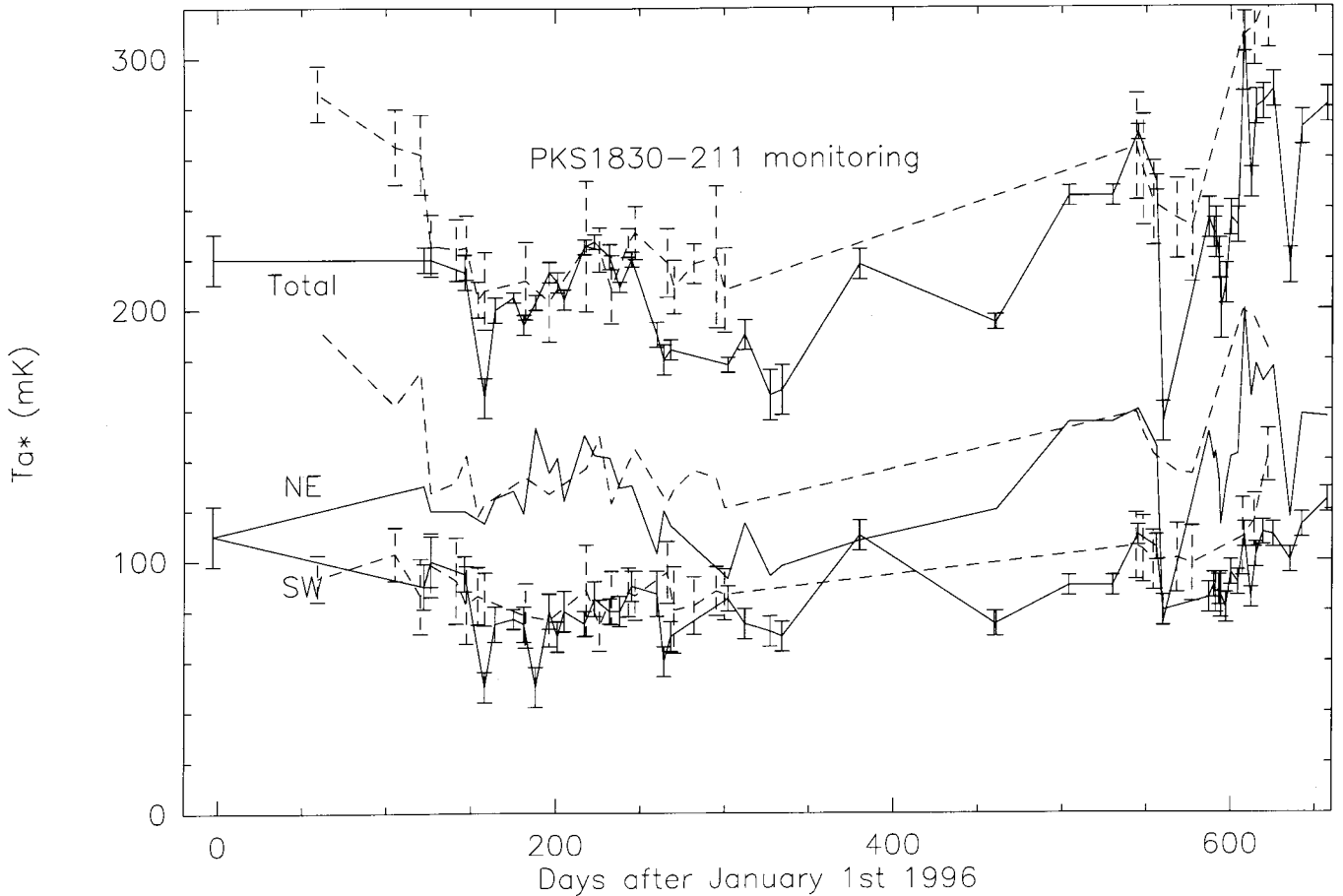


Figure 4: Results of the weekly monitoring of the quasar PKS 1830-211 in the  $\text{HCO}^+(2-1)$  line at  $z = 0.88582$ . The full and dashed lines represent observations done at the IRAM 30-m and SEST 15-m telescopes respectively. From bottom to top the curves are the measure of the continuum level successively of image SW, NE and total. An intrinsic level increase appears from 1996 to 1997 in the two images.

difference between the two path-lengths, which is the product of the light velocity by the time-delay. It is also easy to derive the ratio  $d_1/d_2$  from the relative positions of the two images and the lens on the sky. For a point-source lens, this ratio is obtained directly from the ratio of image-lens angular separations on the plane of the sky. Knowing the difference and the ratio between  $d_1$  and  $d_2$  gives the distance to the source and to the lens, together with a geometrical model of the lens. Given the redshift, a relation between the Hubble constant and the deceleration parameter  $q_0$  follows.

In order to derive a time-delay, individual fluxes from the two images must be measured over a certain period of time. In the two systems where molecular absorption occurs in the lensing galaxy (B0218+357 and PKS1830-211), the image separations are  $0.3''$  and  $1''$ ,

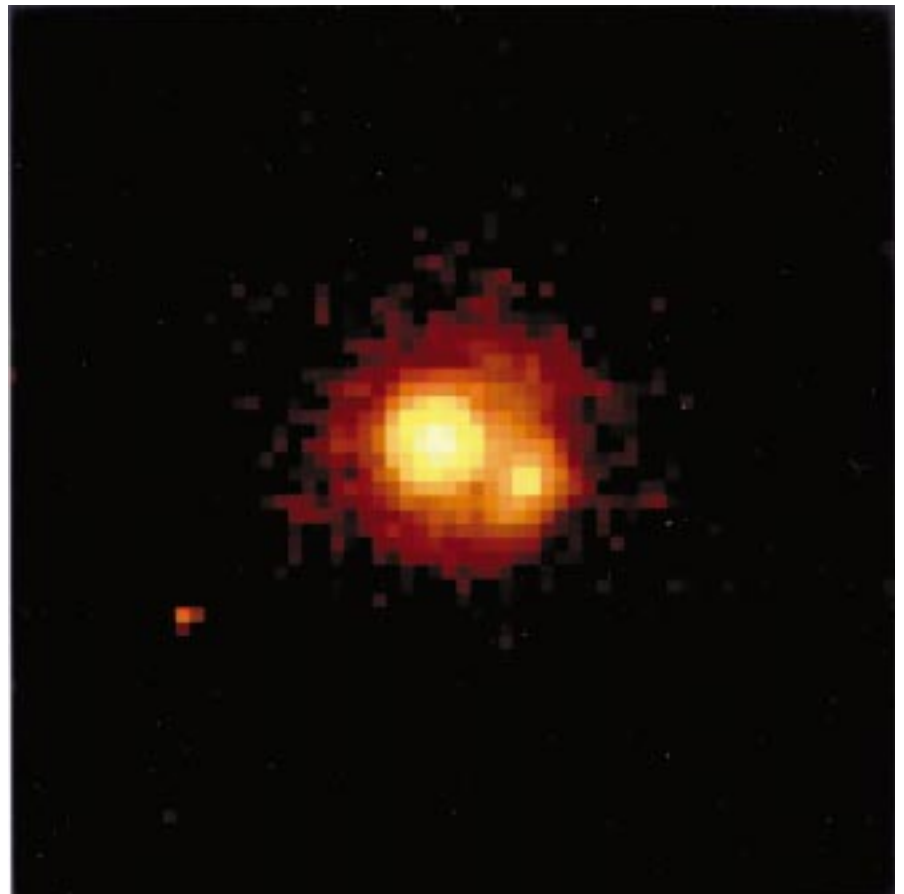


Figure 5: HST F814W image of B0218+357. North is up and east to the left. The pixel scale is 45 mas. The brighter component corresponds to the weak radio core B and the optically weak western component to the brightest radio core A. Comparison of the F555W and F814W bands show no indication of differences in the extinction between the A and B components.

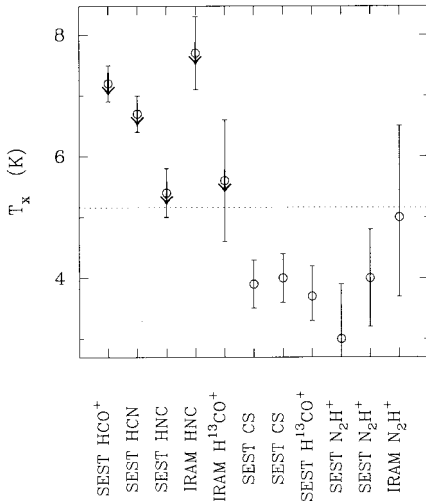


Figure 6: Measure of the excitation temperatures for several molecules shown in abscissa, from two of their rotational transitions. When the lower transition is optically thick, only an upper limit is derived. The horizontal dash line is the cosmic background temperature expected from the big-bang at the redshift of the absorber for PKS1830-211, i.e.  $z = 0.88582$ .

respectively. These are too small to be directly resolved with single-dish telescopes. However, fortuitously enough, in both cases the molecular gas obscures only one of the two quasar images. Therefore in the same beam where the two images are observed together, the depth of the saturated absorption line then directly measures the flux from one image, while the total continuum measures the sum of the fluxes of the two images. This has been checked by resolving the two images with the IRAM Plateau de Bure interferometer (Wiklind & Combes, 1998, *ApJ* in press) for PKS1830-211 and with the VLA for B0218+357 (Menten & Reid, 1996). Interferometer observations are, however, cumbersome to obtain and reduce; good-quality monitoring of the fluxes are in these cases best done using single-dish telescopes, since we do not need to resolve the images.

We have carried out a weekly monitoring of PKS1830-211 quasar since the beginning of 1996 with the IRAM 30-m and SEST 15-m telescopes, the results are plotted in Figure 4. The SEST data have been normalised to be compared with the IRAM ones, both are pretty compatible. However, it is difficult to derive precisely the time-delay, since the intrinsic variations of the quasar have not been of high amplitude during 1996-7, and the atmospheric calibrations introduce unwanted noise in the light curves. The expected time-delay is of the order of a few weeks.

The other lens B0218+357 has a very similar configuration, the flux ratio between the two components is around 3-4 at radio wavelengths, while it is 0.15 in the optical. The main image is

covered by molecular clouds, but not entirely, 4% of the surface remains uncovered and can be seen in the HST image (cf. Fig 5).

## 5. Cosmic Background Temperature

Molecular clouds are usually very cold, with a kinetic temperature of the order of 10-20 K. The excitation temperature of the molecules could be even colder, close to the background temperature  $T_{bg}$ . This is the case when the absorption occurs in diffuse gas, where the density is not enough to excite the rotational ladder of the molecules. This is the case of the gas absorbed in front of PKS1830-211, where  $T_{ex} \sim T_{bg}$  for most of the molecules. The measurement of  $T_{ex}$  requires the detection of two nearby transitions. When the lower one is optically thick, only an upper limit can be derived for  $T_{ex}$ . Ideally, the two transitions should be optically thin, but then the higher one is very weak, and long integration times are required.

The results obtained with the SEST 15-m and IRAM 30-m are plotted in Figure 6. Surprisingly, the bulk of measurements points towards an excitation temperature lower than the background temperature at  $z = 0.88582$ , i.e.  $T_{bg} = 5.20$  K. This could be due to a non-LTE excitation or, possibly, by radiative coupling to a continuum source near the molecular cloud with a colour temperature at millimetre wavelengths lower than  $T_{bg}$ .

## 6. Variation of Fine-Structure Constant

The high spectral resolution of heterodyne techniques, the narrowness of absorption lines and their high redshift make these measurements favourable to try to refine the constraints on the variation of coupling constants with cosmic time, variations that are predicted by for instance the Kaluza-Klein and superstring theories. By comparing the HI 21-cm line (Carilli et al., 1992, 1993) with rotational molecular lines, one can constrain the variations of  $\alpha^2 g_p$ ,  $\alpha$  being the fine-structure constant, and  $g_p$  the proton gyromagnetic ratio. Also, by intercomparison of rotational lines from different molecules, one can test the invariance of the nucleon mass  $m_p$ , since the frequencies are affected by centrifugal stretching.

Recent works on these lines have considerably improved the previous limits (e.g. Potekhin & Varshalovich, 1994). By comparing various optical/UV lines (of H<sub>2</sub>, HI, Cl, SiIV) in absorption in front of quasars, Cowie & Songaila (1995) constrained the variation of  $\alpha^2 g_p m_e / m_p$  to  $4 \cdot 10^{-15}/\text{yr}$ . Varshalovich et al. (1996) from radio lines come to a limit of varia-

tion of  $\alpha^2 g_p$  of  $8 \cdot 10^{-15}/\text{yr}$ . Drinkwater et al. (1997) by a more careful analysis of the same data conclude to  $5 \cdot 10^{-16}/\text{yr}$ . We have also derived a limit from PKS1413+135 and PKS1830-211 data of  $\Delta z / (1+z) < 10^{-5}$ , which yield a corresponding limit of  $2 \cdot 10^{-16}/\text{yr}$  (Wiklind & Combes, 1997b). However, geophysical constraints are in fact superior to all astrophysical ones. Damour et al. (1997) have recently come up with a limit of  $5 \cdot 10^{-17}/\text{yr}$  on  $\alpha$  from the natural fission reactors which operated about  $2 \cdot 10^9$  yr ago at Oklo (Gabon). These results were obtained through analysis of the neutron capture cross section of Samarium, in the Oklo uranium mine.

Notice that we have reached an intrinsic maximum of precision with the astrophysical technique, since the limitation comes from the hypothesis that the various lines compared come from the same material, at exactly the same Doppler velocity along the line-of-sight. This hypothesis is obviously wrong when comparing HI and molecular lines; it is also wrong while intercomparing molecules, or even within lines of the same molecule, since opacity depends on excitation conditions which vary along the line of sight for each transition. The astrophysical techniques do, in contrast to terrestrial methods, test the uniformity of physical constants over large spatial scales.

## References

- Carilli, C.L., Perlman E.S., Stocke J.T. 1992, *ApJ* **400**, L13.
- Carilli, C.L., Rupen, M.P., Yanny, B. 1993, *ApJ* **412**, L59.
- Carilli, C.L., Menten K.M., Reid M.J., Rupen, M.P., Yun M.S.: 1998, *ApJ*, in press.
- Cernicharo, J., et al. 1997, *A&A* **323**, L25.
- Combes, F., Wiklind T. 1995, *A&A* **303**, L61.
- Combes F., Wiklind T., 1996, in *Cold Gas at High Redshift*, eds. M.N. Bremer, P. van der Werf, H.J.A. Röttgering, C.L. Carilli, Kluwer Academic Pub., p. 215.
- Combes, F., Wiklind T. 1997, *ApJ* **486**, L59.
- Combes F., Wiklind T., Nakai N.: 1997, *A&A* **327**, L17.
- Cowie L.L., Songaila A.: 1995, *ApJ* **453**, 596.
- Damour T., Dyson F.: 1997, *Nucl. Phys. B* in press (hep-ph/9606486).
- Drinkwater M.J., Webb J.K., Barrow J.D., Flambaun V.V.: 1997, in "Structure and Evolution of the IGM from QSO Absorption Line Systems" IAP, Paris, ed. P. Petitjean & S. Charlot, in press.
- Greaves J.S., Nyman L.-Å., 1996, *A&A* **305**, 950.
- Lucas R., Liszt H., 1996, *A&A* **307**, 237.
- Menten K.M., Reid M.J.: 1996, *ApJ* **465**, L99.
- Potekhin A.Y., Varshalovich D.A.: 1994, *A&AS* **104**, 89.
- Subrahmanyan R., Narasimha D., Rao A.P., Swarup G.: 1990, *MNRAS* **246**, 263.
- Varshalovich D.A., Panchuk V.E., Ivanchik A.V.: 1996, *Astron. Lett.* **22**, 6.
- Wiklind, T., Combes, F. 1994, *A&A* **286**, L9.
- Wiklind, T., Combes, F. 1995, *A&A* **299**, 382.
- Wiklind, T., Combes, F. 1996a, *Nature*, **379**, 139 - 1996b, *A&A* **315**, 86.
- Wiklind, T., Combes, F. 1997a, *A&A* **324**, 51 - 1997b, *A&A* **328**, 48.